Localization and Characterization of an Orphan Receptor, Guanylyl Cyclase-G, in Mouse Testis and Sperm

Yen-Hua Huang, Chih-Chun Wei, Yueh-Hsing Su, Bo-Tsung Wu, Yi-Yun Ciou, Cheng-Fen Tu, Trevor G. Cooper, Ching-Hei Yeung, Sin-Tak Chu, Ming-Tzu Tsai and Ruey-Bing Yang

Endocrinology 2006 147:4792-4800 originally published online Jul 20, 2006; , doi: 10.1210/en.2005-1476

0013-7227/06/$15.00/0
Printed in U.S.A.

Endocrinology 147(10):4792–4800

doi: 10.1210/en.2005-1476

Localization and Characterization of an Orphan Receptor, Guanylyl Cyclase-G, in Mouse Testis and Sperm

Yen-Hua Huang, Chih-Chun Wei, Yueh-Hsing Su, Bo-Tsung Wu, Yi-Yun Ciou, Cheng-Fen Tu, Trevor G. Cooper, Ching-Hei Yeung, Sin-Tak Chu, Ming-Tzu Tsai, and Ruey-Bing Yang

Department of Biochemistry and Graduate Institute of Medical Sciences (Y.-H.H., C.-C.W., Y.-Y.C.) School of Medicine, Taipei Medical University, Taipei 110, Taiwan; Institute of Reproductive Medicine, University of Muenster, Muenster D-48149, Germany (T.G.C., C.-H.Y.); Institute of Biological Chemistry, Academia Sinica and Institute of Biochemical Sciences (S.-T.C.), College of Science, National Taiwan University, Taipei 106, Taiwan; Institute of Pharmacology, School of Medicine (R.-B.Y.), National Yang-Ming University, Taipei 112, Taiwan; and Institute of Biomedical Sciences (B.-T.W., Y.-H.S., C.-F.T., M.-T.T., R.-B.Y.), Academia Sinica, Taipei 115, Taiwan

We recently identified a novel testis-enriched receptor guanylyl cyclase (GC) in the mouse, designated mGC-G. To further investigate its protein expression and function, we generated a neutralizing antibody specifically against the extracellular domain of this receptor. RT-PCR and immunohistochemical analyses show that mGC-G is predominantly expressed from round spermatids to spermatozoa in mouse testis at both the mRNA and protein levels. Flow cytometry and confocal immunofluorescence reveal that mGC-G is a cell surface protein restricted to the plasma membrane overlying the acrosome and midpiece of the flagellum in mature sperm. Interestingly, Western blot analysis demonstrates that testicular mGC-G is approximately 180 kDa but is subject to limited proteolysis during epididymal sperm transport, resulting in a smaller fragment tethered on the mature sperm surface. On Fluo-3 cytometrical analysis and computer-assisted sperm assay, we found that serum albumin-induced elevation of sperm intracellular Ca^{2+} concentration, protein tyrosine phosphorylation, and progressive motility associated with capacitation are markedly reduced by preincubation of the anti-mGC-G neutralizing antibody. Together, these results indicate that mGC-G is proteolytically modified in mature sperm membrane and suggest that mGC-G-mediated signaling may play a critical role in gamete/reproductive biology. (*Endocrinology* 147: 4792–4800, 2006)

IN SEXUALLY REPRODUCING species, the precise regulation of sperm motility spatially and temporally is essential to achieve fertilization. In the case of marine invertebrates such as sea urchin, sperm motility is activated upon spawning into seawater and can be subsequently modulated by egg-derived peptides (1). These egg-associated peptides (*e.g.* resact or speract) can stimulate sperm motility and metabolism at subnanomolar concentrations and also function as a chemoattractant in a species-specific manner (2, 3). The cross-linking approach using a radiolabeled resact analog identified a membrane guanylyl cyclase (GC) as the receptor in sea urchin (*Arbacia punctulata*) (4). Subsequent cloning of the full-length cDNA revealed that its topology resembled a type I receptor composed of an amino-terminal extracellular domain (ECD), a single membrane-spanning region, an intracellular protein kinase-like domain, and a cyclase catalytic domain at the carboxyl-terminal end (5).

Biochemical and biophysical techniques involving high time resolution (approaching ~10 ms) demonstrated that resact initiates a rapid and transient increase in the concentration of cyclic GMP (cGMP), followed by a transient influx of Ca^{2+} (6). The authors concluded that the primary motor response to the egg-derived chemoattractant was controlled by a cGMP-mediated increase in the Ca^{2+} concentration through, either directly or indirectly, the opening of a cGMP-gated Ca^{2+} channel. Likewise, starfish sperm use a similar sequence of events, but the cAMP increase is absent, again revealing that cGMP is a predominant signaling molecule in promoting Ca^{2+} influx (7). However, analogous ligand-receptor GC interactions have not been identified for sperm activation and chemotaxis in mammals.

To date, seven isoforms of the mammalian receptor GCs, designated GC-A to GC-G, have been cloned (8). These mammalian receptor GCs function in various physiological processes, including regulation of blood pressure, vascular regeneration, phototransduction, and fluid/electrolyte homeostasis (8). GC-A, -B, and -C function as receptors for a number of peptide hormones that stimulate cyclase activity to produce cGMP, analogous to the function of the sea urchin sperm receptor GC. Ligands for the remaining four receptor GCs have yet to be identified (9). Furthermore, none of these genes has been shown convincingly to be expressed in mammalian posttesticular sperm.

GC-G is the last member of the receptor GC family to be identified (10, 11). We have previously identified and demonstrated that mouse GC-G (mGC-G) is highly enriched in

First Published Online July 20, 2006

Abbreviations: $[Ca^{2+}]_i$, Intracellular Ca^{2+} concentration; CASA, computer-assisted sperm assay; cGMP, cyclic GMP; FITC, fluorescein isothiocyanate; GC, guanylyl cyclase; HEK, human embryonic kidney; HM, HEPES medium; mGC-G, mouse GC-G.

***Endocrinology* is published monthly by The Endocrine Society (http://www.endo-society.org), the foremost professional society serving the endocrine community.**

the testis (11). In this report, we further show that mGC-G is a sperm cell surface protein and investigated whether mGC-G plays a role in modulating mouse sperm motility by using an anti-mGC-G-specific neutralizing antibody.

Materials and Methods

Reagents

BSA free from fatty acid, polyvinylalcohol, and pFLAG-CMV1 were from Sigma (St. Louis, MO). Freund's complete and incomplete adjuvants were from Invitrogen (Carlsbad, CA); anti-phosphotyrosine monoclonal antibody (4G10) was from UBI (Lake Placid, NJ); control rabbit IgG, fluorescein isothiocyanate (FITC)-, Cy3-, and horseradish peroxidase-conjugated antirabbit IgG or antimouse IgG were from Jackson ImmunoResearch (West Grove, PA); percoll, protein A column and chemiluinescence detection ECL plus were from Amersham Pharmacia Biotech (Buckinghamshire, UK); Fluo-3 AM was from Molecular Probes (Eugene, OR); anti-fade reagent and Vetabond reagent were from Vector Lab (Burlingame, CA); and ImmunoPure gentle elution buffer was from Pierce (Rockford, IL). All other chemicals were of reagent grade.

Quantitative real-time RT-PCR (TaqMan) analysis

Testicular total RNAs were prepared from mice of defined postnatal ages and subjected to TaqMan analysis. Normalization involved use of glyceraldehydes-3-phosphate dehydrogenase (GAPDH) mRNA levels as described (11). The expression level of GAPDH was constant across testis samples, because the Ct values obtained by TaqMan analysis remained unchanged, at approximately 16.

Expression and purification of the ECD-immunoglobulin fusion protein

The PCR fragment coding for the entire ECD of mGC-G (residues 44–472) was cloned into the mammalian expression vector pFLAG-CMV1 followed by a cDNA fragment of human IgG_1 heavy chain coding for the hinge region and the CH2 and CH3 domains. The resulting expression plasmid was transiently transfected into 293T cells. Twenty hours after transfection, cells were changed to the serum-free medium for an additional 2 d. The mGC-G-IgG chimeric protein secreted into the conditioned medium was purified with use of the protein A column, and bound recombinant protein was eluted with use of the ImmunoPure gentle elution buffer.

Preparation of rabbit polyclonal antisera to mGC-G

A recombinant protein of the ECD (residues 44–472) fused with human IgG Fc fragment was generated as immunogen to raise the anti-GC-G-specific antisera. New Zealand White rabbits were immunized with the recombinant protein. Each rabbit was given an initial sc injection of 0.5 mg of the recombinant protein emulsified in 1 ml of Freund's complete adjuvant. Subsequently, the rabbits received two to three booster injections of 0.25 mg conjugate with Freund's incomplete adjuvant. Antisera were recovered from blood obtained by terminal exsanguinations. The anti-ECD-specific antibody (anti-ECD Ab) was further purified on a column coupled with the recombinant protein containing the mGC-G ECD only to remove the anti-Fc antibody and, therefore, enrich the specific activity for the neutralization. The specificity of the affinity-purified anti-ECD Ab was confirmed by ELISA (data not shown).

Preparation of sperm

Outbred CD-1 mice purchased from Charles River Laboratories (Wilmington, MA) were bred in the Animal Center at Taipei Medical University, School of Medicine. Animals were handled in accordance with institutional guidelines on animal experimentations.

The culture medium used throughout these studies was modified Krebs Ringer bicarbonate HEPES medium (HM) as described previously (12). In brief, modified HM contains 120.0 mM NaCl, 2.0 mM KCl, 1.20 mM $MgSO_4 \cdot 7\,H_2O$, 0.36 mM NaH_2PO_4, 15 mM $NaHCO_3$, 10 mM HEPES, 5.60 mM glucose, 1.1 mM sodium pyruvate, and 1.7 mM $CaCl_2$. Polyvinylalcohol (1 mg/ml) was added to serve as a sperm protectant (13). The pH of the medium was adjusted to 7.3–7.4 with humidified air/CO_2 (95:5) in an incubator at 37 C for 48 h before use (14). An amount of 90% Percoll was made isotonic by adding 1 volume of 10× HM to 9 volumes of Percoll. The 90% Percoll was further diluted with 1× HM to give 20, 40, 60, and 80% Percoll solution, which was humidified with air/CO_2 (95:5) in an incubator at 37 C for 24 h before use. Mature mouse sperm were harvested by a swim-up procedure from the cauda epididymis and isolated either by centrifugation at 50 × *g* for 5 min, or with a 20–80% Percoll gradient by centrifugation at 275 × *g* at room temperature for 30 min, which is especially for intracellular Ca^{2+} concentration ($[Ca^{2+}]_i$) detection and computer-assisted sperm assay (CASA). The sperm used in the present study were viable and progressively motile.

Tissue lysate preparation and Western blot analysis

Mouse testis or sperm were prepared by homogenization in modified RIPA buffer (25 mM HEPES, 125 mM NaCl, 1% Triton X-100, 0.5% sodium deoxycholate, 0.1% sodium dodecylsulfate, 10 mM EDTA) supplemented with protease inhibitor cocktail (Sigma). For the most complete extraction of proteins, mouse sperm were directly lysed and boiled in Laemmli buffer. Tissue and cell debris were removed by centrifugation at 10,000 × *g* for 20 min at 4 C. Twenty micrograms of total protein were loaded on mini SDS-PAGE for Western blot analysis with anti-ECD Ab (10 μg/ml), followed by peroxidase-conjugated goat antirabbit IgG as previously described (15).

Detection of protein tyrosine phosphorylation

Sperm (5×10^6 cells/ml) were preincubated with anti-ECD Ab (20 μM) or rabbit IgG (20 μM) or HM (control medium) at 37 C for 15 min, and then equal volumes of BSA (0.6%) with or without the anti-ECD-Ab (20 μM) or rabbit IgG (20 μM) was added into the specified culture medium. For the control group, an equal volume of HM was added. The final concentration of BSA was 0.3%, but the concentration of the anti-ECD Ab or rabbit IgG remained unchanged. The sperm were further incubated at 37 C for 75 min, and the cell lysates were prepared for Western blot analysis as described previously (12).

Histological and cytological studies

For histological analysis, testis tissues were fixed in freshly prepared Bouin's solution [0.2% picric acid, 2% formaldehyde in PBS (vol/vol)] overnight, and then dehydrated in ethanol, infiltrated, and embedded in paraffin. Each tissue section (4 μm) was mounted on a Vetabond reagent-coated slide and then dried at 55 C. Paraffin of testis sections was removed by dipping in xylene, and the sections were rehydrated through a solution of alcohol to distilled water gradient. The rehydrated sections underwent a modified antigen retrieval process to improve the immunohistochemical staining (16). Briefly, after deparaffination, tissue sections were heated in an antigen unmasking working solution (Vector Lab) to 100 C for 10 min in a microwave, and then cooled to room temperature. After the retrieval process, testis slides were washed in PBS buffer to remove the unmasking solution and then incubated in a blocking solution [5% nonfat skimmed milk in PBS (vol/vol)] at 25 C for 1 h. After a 1-h incubation, the section was washed with PBS containing 0.05% (vol/vol) Tween 20 (PBST) four times for 15 min each. The rabbit anti-ECD Ab was used as the primary antibody (10 μg/ml), and Cy3-conjugated antirabbit IgG served as the secondary antibody (1:1000). After a 1-h incubation for each antibody, the sections were washed with PBST four times. The specimens on a slide were covered with anti-fade reagent and photographed by use of a microscope equipped with epifluorescence (AH3-RFCA; Olympus, Melville, NY).

For confocal cytological analysis, freshly prepared cauda epididymal sperm were fixed in 3.7% paraformaldehyde/PBS for 30 min and smeared on a glass slide. The specimens were then incubated in the blocking solution for 1 h, then incubated with the anti-ECD Ab (10 μg/ml) as the primary Ab and FITC-conjugated antirabbit IgG as the secondary Ab (1:1000). The sperm on a slide were covered with anti-fade reagent and visualized on confocal fluorescent microscopy (Bio-Rad MRC-1000; Bio-Rad, Hercules, CA).

Flow cytometry

The intracellular calcium ion concentration, $[Ca^{2+}]_i$, of sperm was determined with use of fluo-3 AM by flow cytometry (FACScan; BD, San Jose, CA). In brief, Percoll-separated sperm were loaded with fluo-3 AM (10 μM) at 37 C for 10 min. After incubation, sperm were washed twice with modified HM at 50 $\times$ *g* for 5 min to remove any free fluo-3 AM. Fluo-3 AM-loaded sperm (10^6 cells/ml) were preincubated with the anti-ECD Ab (0–20 μM), rabbit IgG (20 μM), or HM (control medium) at 37 C for 15 min, and then equal volumes of BSA (0.6%) with or without the anti-ECD-Ab (0–20 μM) or rabbit IgG (20 μM) were added into the specified culture medium. In the control group, an equal volume of HM was added. The final concentration of BSA was 0.3%, but the concentration of the anti-ECD Ab or rabbit IgG remained unchanged. The sperm were further incubated at 37 C for 45 min, and $[Ca^{2+}]_i$ content was analyzed by flow cytometry. The fluorescence of fluo-3 was excited at 488 nm and measured via a 515- to 540-nm filter. Photomultiplier tube voltages and gains were set to optimize the dynamic range of the signal. The fluorescence intensity of sperm was quantified for 10,000 individual sperm cells.

To determine the surface expression of mGC-G, Percoll-separated sperm were incubated with or without rabbit anti-ECD Ab (10 μg/ml) in blocking solution (2% FBS in PBS) at 4 C for 30 min. After the primary antibody incubation, the sperm cells were washed with HM, then incubated with FITC conjugated antirabbit IgG (1:100 in blocking solution) as the secondary antibody. The sperm cells were washed with HM again, and then fixed by 2% ice-cold paraformaldehyde/PBS and analyzed by flow cytometry.

Assay of sperm motility by CASA

Percoll-separated sperm (5×10^6 cells/ml) were preincubated with the anti-ECD Ab (7 μM), rabbit IgG (7 μM), or HM (control) at 37 C for 15 min. After the incubation, an equal volume of HM or BSA (0.6%) in the presence or absence of the anti-ECD-Ab (7 μM) or rabbit IgG (7 μM) was added (labeled as "BSA", "anti-ECD + BSA", or "rabbit IgG + BSA"), and this time point was designated as time 0. The final concentration of BSA was 0.3%, but the concentration of the anti-ECD Ab or rabbit IgG remained unchanged. The sperm were further incubated at 37 C for 30 min. At least 200 sperm cells were analyzed to monitor sperm movement characteristics. The parameters associated with the motility of sperm under different experimental conditions were determined by CASA with use of a sperm motility analyser (IVOS version 10; Hamilton-Thorne Research, Beverly, MA). A 7.0-μl sample was placed in a 10-μm deep Makler chamber at 37 C. The analyser was set as described previously (17). The accuracy of the machine in identifying motile and immotile spermatozoa was validated by use of the playback function. Fifteen fields were assessed for each sample.

Statistical analysis

All experiments were repeated at least three times with three different pooled sperm samples from four or five male mice. The data are expressed as mean ± SD. Difference in means was assessed by one-way ANOVA, followed by the Tukey-Kramer multiple comparisons test.

Results

Postnatal developmental profile of mGC-G in mouse testis

We previously demonstrated that mGC-G mRNA is highly and exclusively expressed in the testis (11). To determine whether mGC-G expression is restricted to a particular cell type or stage in testis, we then performed real-time quantitative RT-PCR (TaqMan) on testicular cDNAs derived from postnatal male mice from 1–28 d old and up to adulthood (8–10 wk old). As shown in Fig. 1, mGC-G expression was first detected on the testis at d 18 of postnatal development and thereafter increased progressively. The onset of mGC-G expression at d 18 and subsequent stages coincides with the formation of spermatids, which suggests that mGC-G is expressed in postmeiotic germ cells in the mouse testis.

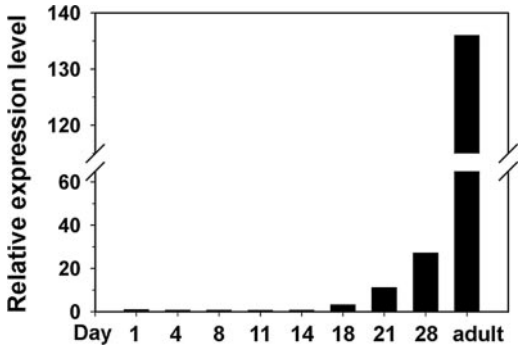

FIG. 1. Postnatal expression profile of mGC-G in mouse testis. Mouse testes were collected at various developmental stages ranging from d 1 postpartum to adult (8–10 wk old). The testis developmental profile of mGC-G was determined by quantitative real-time RT-PCR analysis. Expression levels were normalized to that of GAPDH. The expression level of GAPDH appeared constant throughout the testis samples, because the Ct values obtained by TaqMan analysis remain unchanged at approximately 16. Note that the mRNA expression profile of mGC-G coincides with the appearance of spermatids.

Generation of anti-mGC-G-specific antibody (anti-ECD Ab)

To further confirm the protein expression of mGC-G in testis, we raised polyclonal Ab (anti-ECD) against mGC-G using a soluble chimeric protein consisting of the ECD of the receptor fused with the Fc portion of human IgG as described (18, 19). The anti-ECD serum was purified further by the column conjugated with the ECD recombinant protein to remove anti-Fc antibodies contaminated in the anti-ECD Ab. The specificity of the purified anti-ECD Ab was confirmed by ELISA with human IgG used as the antigen; *i.e.* the purified anti-ECD Ab failed to react with human IgG, whereas the Ab before the purification step showed significant reactivity with the antigen (data not shown). These results indicate that a further step of affinity purification was extremely effectively in removing anti-Fc Ab from the anti-ECD Ab. Consistently, the anti-ECD Ab could specifically recognize the recombinant mGC-G protein expressed in human embryonic kidney (HEK)-293T cells by Western blotting (Fig. 2) or flow

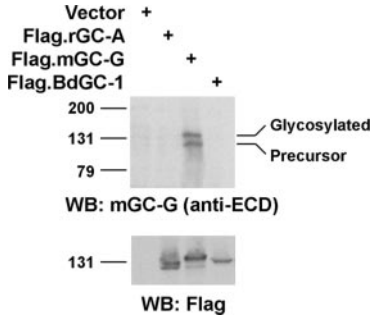

FIG. 2. Specificity of anti-mGC-G Ab. A polyclonal rabbit Ab (anti-ECD) was raised specifically against the entire ECD of mGC-G. A number of different receptor GCs were expressed in HEK-293T cells and subjected to Western blot analysis with the anti-ECD Ab. The anti-ECD Ab recognized only the mGC-G protein but not two other receptor GCs [GC-A or a fly receptor GC, BdGC-1 (20)]. The expression levels of each recombinant GC protein were confirmed by anti-Flag Western blot analysis (*bottom panel*). Preincubation of antibody with the respective immunizing antigen abolished the specific immunoreactive bands, which demonstrates the specificity of these antibodies (data not shown).

cytometry (data not shown) but not other receptor GCs, such as GC-A or an insect receptor GC (BdmGC-1) (20).

Localization of mGC-G in the mouse testis

We then examined the expression pattern of mGC-G by indirect immunofluroscence on testicular sections of adult mice using this anti-mGC-G-specific Ab (anti-ECD). Overall, the staining pattern for the anti-ECD Ab varied among individual seminiferous tubules depending on the stage of spermatogenesis (data not shown). As shown in Fig. 3, the anti-ECD immunoreactivity is predominantly associated in sperm from round spermatids to spermatozoa. In addition, we also consistently observed staining in interstitial Leydig cells (Fig. 3B, *arrowhead*). However, spermatogonia, Sertoli cells, and spermatocytes were not labeled (Fig. 3B). Preincubation of the antibody with the respective immunogen (data not shown) or the control rabbit IgG (Fig. 3C) resulted in no staining, thus demonstrating the specificity of the immunofluorescent staining in the testis.

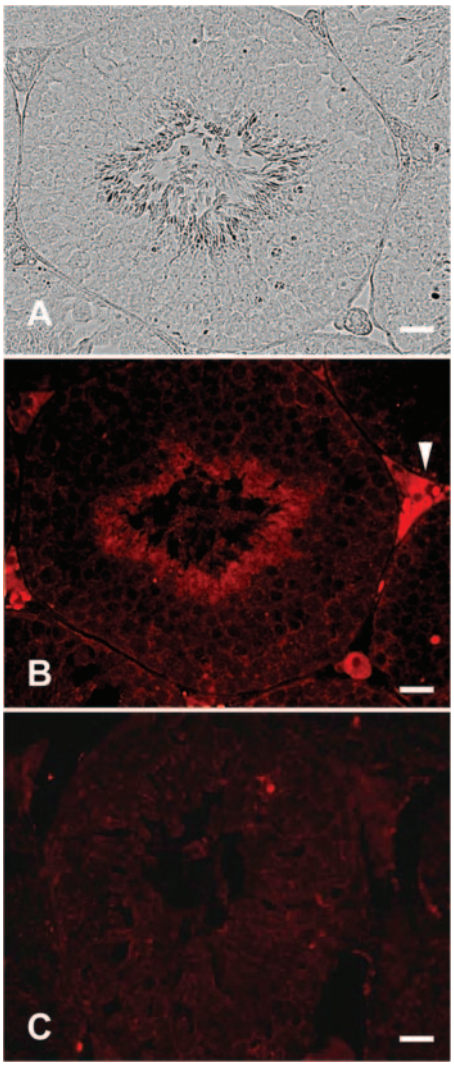

FIG. 3. Immunofluorescent localization of mGC-G in mouse testis. Cross-sections of seminiferous tubules were stained with antibody specific for mGC-G (anti-ECD). B, The immunoreactivity was predominantly detected in sperm from round spermatids to spermatozoa. Note that the signal is also seen in intertubular Leydig cells (*arrowhead*). The corresponding phase-contrast image is shown in A. C, No staining is observed with control rabbit IgG. *Bars*, 50 μm.

Spatial distribution of mGC-G in mature sperm

Given that mGC-G protein is expressed in spermatids, we next examined the precise cellular distribution of mGC-G in mouse sperm by using the anti-ECD Ab in conjunction with light or confocal immunoflurescence microscopy and flow cytometrical analysis. Cauda epididymal sperm were freshly prepared by a swim-up method to obtain mainly motile, uncapacitated, acrosome-intact cells. As shown in Fig. 4A, indirect immunofluorescence revealed that anti-ECD Ab produced intense immunostaining in the anterior region of the sperm head and in the midpiece of the flagellum. A weaker fluorescence signal was occasionally observed in the end piece (Fig. 4A, *arrows*). The omission of primary antibody resulted in no significant fluorescent signal (data not shown), which confirmed that the results did not reflect nonspecific binding of secondary antibody. In addition, preadsorption with immunogen was used routinely as a negative control and resulted in elimination of fluorescence.

We then used confocal microscopy and flow cytometry to determine mGC-G localized on the cell surface of sperm. The confocal microscopic observation allows for clear separation of the fluorescence staining of plasma membranes, nuclear, or cytoplasmic compartments without interference from overlapping cellular structure as observed by epifluorescence microscopy. Paraformaldehyde-fixed, nonpermeablized mouse cauda epididymal sperm were immunostained with the anti-ECD Ab and examined by confocal microscopy. As shown in Fig. 4, B and C, fluorescent reactivity was clearly associated along the cell surface within the plasma membranes overlying the acrosome and the midpiece of the flagellum. Consistent with this finding, flow cytometry revealed a right-shift of the entire sperm cell population on incubation with the anti-ECD Ab followed by an FITC-conjugated secondary Ab (Fig. 4D). Together, these data clearly demonstrate that mGC-G is a cell surface protein expressed in mouse sperm.

Identification of testicular or sperm mGC-G by Western blot analysis

To further validate the molecular identity of mGC-G immunoreactivity, we then performed Western blot analysis with protein extracts from mouse testis and sperm. As shown in Fig. 5A, the anti-ECD Ab recognized a testis-specific protein with an apparent molecular mass of 180 kDa, which is not seen in lysates from mouse lung, kidney, or heart (supplemental Fig. 1). This mass exceeded that of recombinant protein expressed in HEK-293T cells by more than 20 kDa, which implies that additional posttranslational modifications such as glycosylation occur *in vivo*. In support of this notion, Western blot analysis revealed that treatment of testis membranes with PNGaseF reduced the molecular mass of testicular mGC-G to approximately 120 kDa, which is consistent with the size of the deglycosylated core protein (supplemental Fig. 2). Again, these results confirm that mouse testis GC-G contains predominantly *N*-linked oligosaccha-

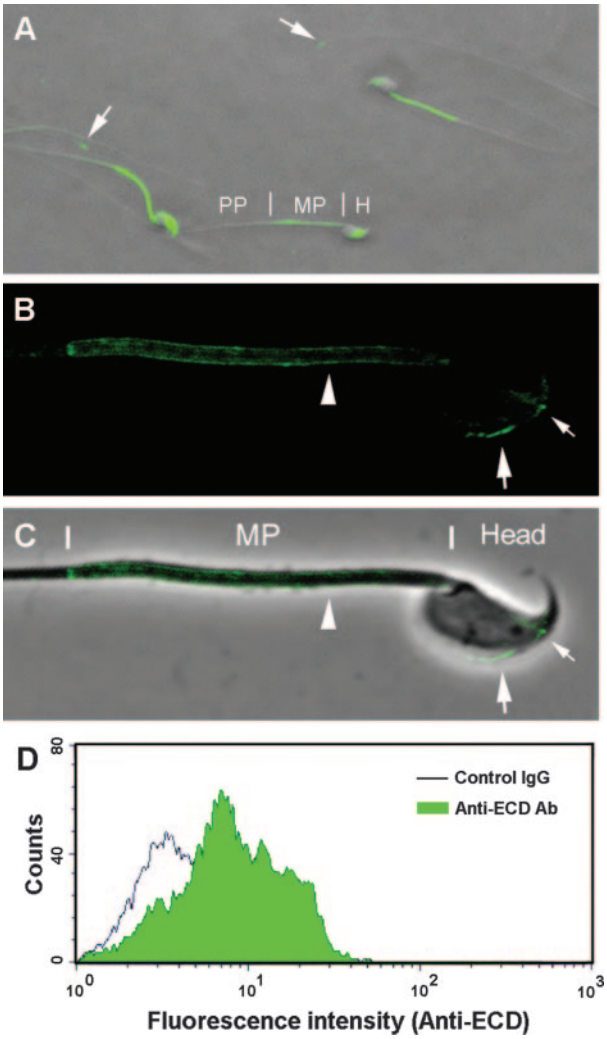

FIG. 4. Localization of mGC-G in mouse cauda epididymal sperm with the anti-ECD antibody. A, Light microscopic localization of mGC-G. Photograph shown is a merge of phase constrast and epifluorescence (FITC) images of mGC-G localization by immunofluorescence on paraformaldehyde-fixed cells. Note the intense labeling on the anterior portion of the head and midpiece of all cells. Magnification, ×400. B and C, Immunolocalization of mGC-G to the plasma membrane of the head and midpiece of mature mouse sperm. Confocal immunofluroscence images shown for paraformaldehyde-fixed, nonpermeabilized mouse cauda epididymal sperm stained with the anti-ECD antiserum. Confocal fluorescence image (B) merged with the phase-contrast image is shown in C. Intense immunofluroscence is highly associated with the plasma membrane overlaying the acrosome (*arrow*), the anterior head region (*small arrow*), and on the midpiece (*arrowhead*) of mouse sperm. H, Head; MP, midpiece; PP, principle piece of the flagellum. Magnification, ×1000. D, Sperm surface expression of mGC-G by flow cytometrical analysis. Mature sperm were collected and stained with anti-ECD Ab (10 μg/ml) or control rabbit IgG, followed by an FITC-conjugated antirabbit IgG secondary Ab, and then analyzed by FACS analysis.

ride chains. In contrast, the same Ab detected a major signal of reduced molecular mass at 48 kDa in cauda epididymal sperm (Fig. 5B and supplemental Fig. 3). Most importantly, the anti-ECD Ab preabsorbed with immunogen resulted in no immunoreactive staining, which again supports the specificity of Ab binding.

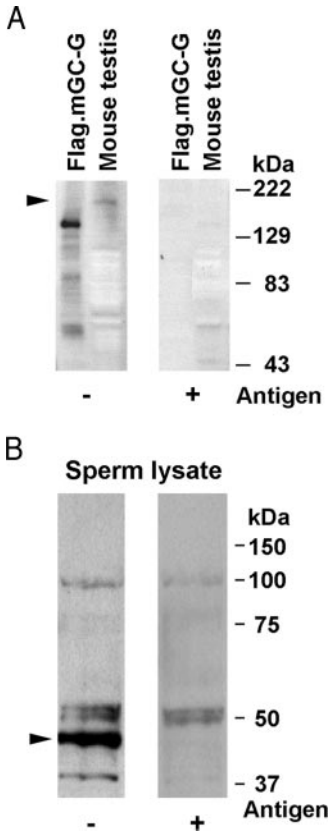

FIG. 5. Identification of testicular or sperm mGC-G by the anti-ECD Ab. Mouse testis (A) or sperm protein extracts (B) (20 μg each) were separated by SDS-PAGE and transferred to a polyvinylidene difluoride membrane. After incubation with affinity-purified anti-ECD Ab (10 μg/ml), a major protein of 180 or 48 kDa was detected from the testis or sperm lysate (*arrows*), respectively. The testis-specific band is not seen in other mouse tissue lysates including lung, kidney, or heart (supplemental Fig. 1). Flag-epitope tagged mGC-G (Flag-.mGC-G) expressed in HEK-293T cells was used as a positive control. When the anti-ECD Ab was preincubated with a 100-fold excess of its corresponding antigen (+) before addition to the blots, the Ab failed to detect the specific immunoreactive band, which confirms the specificity of Ab binding.

Functional characterization of mouse sperm GC-G

Given its cell surface localization on the plasma membranes of the head and the midpiece of mature sperm, mGC-G might play an important role in sperm biology. Mammalian sperm produced in the testes are immobile first and acquire the ability to swim forward during their transport through the epididymis (21). After ejaculation or dilution into a defined medium, sperm become motile, yet lack fertilizing competence. Sperm must undergo an additional maturation process, termed capacitation, before they can fertilize an egg in the female genital tract. Sperm capacitation is a prerequisite for the acrosome reaction [*i.e.* release of matrix-digesting enzymes enabling sperm penetration through the extracellular matrix coat of the egg (zona pellucida)]. An increase in cellular Ca^{2+} concentration is involved in the regulation of the aforementioned sperm processes, including motility (22, 23), chemotaxis (24, 25), capacitation (26), and the acrosomal reaction (21).

Serum albumin is an abundant protein in the female re-

productive tract, and it is thought to play a role in stimulating sperm processes and fertilization *in vivo* (21). BSA, its bovine equivalent, has been widely used to induce the $[Ca^{2+}]_i$ influx for the study of subsequent motility, capacitation and acrosome reaction of mammalian sperm (12, 21, 27). We thus used the BSA-induced $[Ca^{2+}]_i$ elevation as an assay to evaluate whether mGC-G participates in sperm processes. The relative $[Ca^{2+}]_i$ reflected by the Ca^{2+}-dependent changes in fluroscence intensity of Fluo-3 (a calcium indicator dye) was then determined by flow cytometry. Because of the lack of a known ligand or specific inhibitor for mGC-G, we used the anti-ECD Ab specifically against the entire ECD of this receptor as a neutralizing reagent in our studies (see Fig. 2). This type of neutralizing Ab has been successfully applied to block the signaling functions of other receptor GCs (18, 19, 28).

Fluo-3-loaded sperm were first induced for Ca^{2+} influx by BSA (0.3%) in the absence or presence of preincubation with the anti-ECD Ab or rabbit IgG at various concentrations. As shown in Fig. 6, incubation with BSA alone substantially increased the $[Ca^{2+}]_i$ level, compared with the control sperm. Interestingly, preincubation followed by treatment with the anti-ECD Ab significantly inhibited the BSA-induced elevation of $[Ca^{2+}]_i$ in a dose-dependent manner, whereas an irrelevant rabbit IgG had no effect (Fig. 6). In addition, we have verified that incubation of the anti-ECD Ab alone (up to 20 μM) had no effect on the basal level of $[Ca^{2+}]_i$ (88 ± 12% *vs.* 100%; anti-ECD Ab *vs.* control). Together, these results suggest that mGC-G may be involved in the upstream signaling cascade leading to increased cellular Ca^{2+} concentration during sperm activation.

We then determined whether the anti-ECD Ab affected BSA-induced protein tyrosine phosphorylation associated with sperm capacitation. Supplemental Fig. 4 shows the protein tyrosine phosphorylation patterns of epididymal sperm after incubation with 0.3% BSA in the absence or presence of the anti-ECD Ab or the control IgG at 37 C for 90 min, respectively. As shown, tyrosine phosphorylation of proteins in the range of 40–120 kDa was greatly enhanced in the BSA-treated sperm (lane 3), compared with that of the control cells. However, preincubation of the anti-ECD Ab markedly suppressed the BSA-induced phosphorylation, whereas the control IgG had no effect (lanes 4 and 5). Together, these data suggest that mGC-G may also play a role in sperm capacitation.

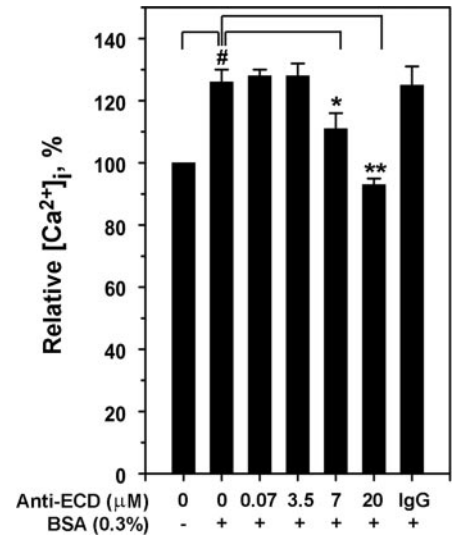

FIG. 6. Effect of anti-ECD Ab on the BSA-induced elevation of $[Ca^{2+}]_i$ in mouse mature sperm. Fluo-3-loaded sperm were preincubated in HM alone, or supplemented with either the anti-ECD Ab (0–20 μM) or rabbit IgG (20 μM) for 15 min, followed by an additional 45-min incubation of BSA (0.3% in final concentration supplement with rabbit IgG or anti-ECD Ab) to induce the Ca^{2+} influx (see *Materials and Methods*). Relative $[Ca^{2+}]_i$ in sperm samples was measured by fluorescence intensity of Fluo-3 (a calcium indicator dye) via flow cytometry. Experiments were performed three times with similar results. #, $P < 0.001$; *, $P < 0.01$; **, $P < 0.001$.

To further dissect the molecular step at which mGC-G participates in the capacitation, we then examine whether mouse sperm isolated in HM (without bicarbonate) are able to mount a cAMP response by bicarbonate addition during the first minute of stimulation in the absence or the presence of the anti-ECD Ab. As shown in supplemental Fig. 5, whereas bicarbonate stimulates a marked elevation of cAMP in sperm, addition of the anti-ECD Ab or control IgG has no effect on the cAMP level. These results suggest that mGC-G may function downstream of or parallel with soluble adenylyl cyclase and upstream of tyrosine phosphorylation events during capacitation.

It has been well documented that sea urchin sperm receptor GCs modulate sperm motility and chemotaxis in response to egg-associated factors (1, 2). However, analogous ligand-receptor interactions have not been described in mammals. Because CASA is widely used to evaluate mammalian sperm parameters such as motility and velocity, we used CASA to assess the effect of the anti-ECD Ab on the motility-promoting activity of BSA in mouse sperm. As shown in Table 1, without preincubation with the anti-ECD Ab, BSA significantly induced sperm motility (defined as the proportion of motile cells) at 30 min incubation, compared with the control sample. Interestingly, preincubation with the anti-ECD Ab greatly suppressed the BSA-induced motility to a level comparable to that in the control sample, whereas an irrelevant rabbit IgG had no effect on BSA-induced motility (Table 1). Most importantly, the inhibitory effect of the anti-ECD Ab on BSA-induced activity was not

TABLE 1. Effect of the anti-ECD Ab on BSA-induced sperm progressive motility

Motility parameters	Control	BSA	Anti-ECD + BSA	IgG + BSA
Motility (%)	72 ± 3.0	83 ± 0.7[a]	69 ± 3.0[b]	84 ± 4.0[c]
VAP (μm/sec)	109 ± 2.3	125 ± 3.9[a]	105 ± 5.0[b]	118 ± 6.0[c]
VSL (μm/sec)	70 ± 5.0	86 ± 3.9[a]	68 ± 3.6[b]	86 ± 5.0[c]
VCL (μm/sec)	197 ± 4.8	222 ± 7.0[a]	192 ± 6.0[b]	218 ± 10.0[c]

Mature mouse sperm were pre-incubated with HM (Control), the anti-ECD antibody (7 μM), or rabbit IgG (7 μM) for 15 min, followed by BSA (0.3%) treatment for additional 30 min as described in Fig. 6. At the end of incubation, the sperm progressive motility was evaluated by CASA. Incubation with the anti-ECD antibody (7 μM) alone has no significant effect on sperm motility as compared to control (65 *vs.* 72%). VAP, Average path velocity; VSL, straight line velocity; VCL, curvilinear velocity.

[a] Difference from control group is significant with $P < 0.05$ (Control *vs.* BSA).

[b] Difference from the BSA treatment alone is significant with $P < 0.01$ (BSA *vs.* anti-ECD + BSA).

[c] Difference from the BSA treatment alone is not significant.

caused by enhanced sperm agglutination. Sperm treated with BSA in the presence or absence of the anti-ECD Ab or rabbit IgG did not enhance the proportion of head-to-head agglutinated spermatozoa (data not shown). In addition, the anti-ECD Ab treatment resulted in reduced BSA-induced forward velocity evaluated by sperm kinematic parameters including average path velocity (the distance traveled along a smoothed average path divided by the elapsed time), straight line velocity (VSL, the straight-line distance from the beginning to the end of a track divided by the time taken) and curvilinear velocity (the total distance traveled by the sperm along its curvilinear path divided by the elapsed time) (Table 1).

Discussion

In the present study, we demonstrate that mGC-G is a mouse sperm cell surface receptor and uncover its role in the functional cascade that leads to sperm motility. As shown in Figs 1 and 3, the mRNA expression of mGC-G is broadly in agreement with its protein expression in sperm from round spermatids to mature sperm. In a recent study, GC-A was shown to be expressed in round and elongated spermatids in the rat testis by radioligand receptor labeling and immunological approaches; however, its expression in cauda epididymal sperm was not reported (29). Although the sea urchin sperm-receptor GC localizes to the entire length of the flagellum (30), we found that mGC-G is restricted to the midpiece of the flagellum and the head region. Confocal immunofluroscence and flow cytometry confirmed that mGC-G is localized on the plasma membrane surrounding the midpiece and the head plasma membrane covering the acrosome (Fig. 4).

One interesting observation from this study is that Western blot analysis provided evidence for proteolytic processing of mGC-G during epididymal sperm transport (Fig. 5). Similar cellular distributions and proteolytic modifications have been reported for a number of sperm membrane proteins, such as adenylyl cyclases (31) or fertilin α/β subunits (32). In addition, a similar proteolytic process has been described for GC-C, an intestinal receptor for *Escherichia coli* heat-stable enterotoxins or peptide ligand guanylin/uroguanylin (33, 34). In these studies, the proteolytic fragments of GC-C were proposed to be surface bound via inter/intramolecular disulfide bridges. Moreover, the proteolytic cleavage of GC-C did not seem to impair the functional coupling of this receptor to the cyclase activity in rat intestinal membranes. Likewise, an mGC-G fragment tethered on the sperm surface may use similar membrane-anchoring and cyclase-coupling mechanisms. On the basis of the reduced molecular mass of mGC-G, proteolytic cleavage likely occurs within its ECD in the sperm membrane. However, the exact cleavage site and the identity or the activation mechanisms of the relevant mGC-G processing components remain to be further investigated.

Because of lack of a known activator and specific pharmacological reagents, we produced a neutralizing Ab specifically against the ECD of mGC-G for functional studies. A similar approach has been repeatedly used to generate functionally blocking Abs for GC-A, -B, or -C (18, 19, 28). As shown in Fig. 6, preincubation with this neutralizing Ab (anti-ECD) indeed inhibited BSA-induced elevation of $[Ca^{2+}]_i$ in mouse sperm in a dose-dependent manner. In addition, preincubation of the anti-ECD Ab greatly reduced the proportion of motility, forward velocity, and the protein tyrosine phosphorylation associated with sperm capacitation induced by BSA (Table 1 and supplemental Fig. 4). The change in $[Ca^{2+}]_i$ level coincides with the intensity of capacitation-associated protein tyrosine phosphorylation in sperm (*cf.* Fig. 6 and supplemental Fig. 4). Together, these results imply that mGC-G may play a role in the functional cascade leading to capacitation and motility. Because mGC-G exclusively localizes to the anterior and acrosomal region of the sperm head of mature mouse sperm, this receptor may also be involved in a signaling cascade leading to acrosome reaction. We currently are addressing these questions through a more conclusive gene-targeting methodology to further unravel the physiological functions of mGC-G in the murine system.

Our recent study showed that incubation of either the anti-ECD Ab or control rabbit IgG alone resulted in no change in the basal levels of intracellular cGMP concentrations both in mouse sperm ($\sim$1 pmol/10^7 sperm) or in HEK-293T cells stably expressing mGC-G ($\sim$190 pmol/10^5 cells). However, the sperm cGMP levels may dynamically change during the activation process and local subcellular effects caused by compartmentalization of mGC-G may not be detected by whole cell content measurements.

BSA is believed to function as a sink to remove cholesterol from the sperm plasma membrane (35, 36). Recent studies further demonstrated that BSA-mediated cholesterol efflux increases the overall membrane fluidity of the sperm plasma membrane, causing a shift of the raft-associated proteins to the nonraft domain to initiate a signaling cascade leading to subsequent sperm processes (37, 38). Although the molecular mechanism by which the anti-ECD Ab modulates the BSA-induced increase in $[Ca^{2+}]_i$ in mouse sperm is currently unclear, the anti-ECD Ab binding may limit the BSA-mediated redistribution and thus signaling of membrane mGC-G, resulting in a downstream reduction in $[Ca^{2+}]_i$ elevation and sperm motility. However, further studies are required to validate this hypothesis. Interestingly, the membrane proteins that control Ca^{2+} entry [cation channel of sperm (CatSper1 and CatSper2)] (22, 39–41) or Ca^{2+} extrusion [plasma membrane Ca^{2+} ATPase 4 (PMCA4)] (42, 43) have been recently identified to be specifically expressed in spermatozoa and linked to sperm motility. It remains to be determined whether mGC-G is indeed functionally coupled with these Ca^{2+} influx or efflux regulatory proteins.

Our previous study showed that all peptide ligands known to mammalian receptor GCs failed to stimulate mGC-G activity (11); therefore, mGC-G remains an orphan receptor. Because of its sperm surface expression, if mGC-G is a receptor, ligand(s) may reside within the luminal fluids of the male or female reproductive tracts. However, we do not exclude the presence of a surface-tethered ligand that functions in an autocrine fashion to activate mGC-G during sperm activation. Additional studies are required to examine the existence of such a sperm-associated activator for mGC-G.

In addition to the Ca^{2+} influx and efflux regulatory pro-

teins in sperm, a number of target proteins for cGMP, such as cGMP-dependent protein kinase (PKG) (44, 45), PKG-anchoring protein (46), and cGMP-gated Ca^{2+} channel (47, 48), are also present in male germ cells, which raises the possibility that these proteins may represent the direct downstream target molecules for mGC-G. Alternatively, mGC-G may use other signaling mechanisms in addition to cGMP synthesis. In support of this possibility are many examples of signaling proteins possessing the kinase-like domain similar to those found in the intracellular domain of mGC-G (49).

We also observed the expression of mGC-G in the interstitial Leydig cells in addition to the predominant intratubular distribution in the mouse testis (Fig. 3). This finding raises the possibility that mGC-G may also play an important role in this type of somatic cell. Interestingly, production of testosterone by Leydig cells has been shown to be regulated by GC-A-mediated cGMP elevation through its peptide ligand, atrial natriuretic peptide, both *in vitro* and *in vivo* (50, 51). The germ cell-enriched expression of mGC-G in the mouse testis is completely distinct from a broader tissue expression by its rat orthologue [*i.e.* in the lung, small intestine, skeletal muscles, and kidney (10)]. Despite multiple attempts, we were unable to detect the expression of rat GC-G in the testis even by a more sensitive method of RT-PCR amplification. Thus, it remains to be determined whether the male germ cell-specific expression of GC-G is unique to the mouse or exists in other species as well.

In summary, we have demonstrated that mGC-G is a novel sperm surface receptor and possibly functions, similar to its sea urchin counterpart, in the early signaling event that regulates the Ca^{2+} influx/efflux and subsequent motility response in sperm. A further understanding of the functions of this sperm receptor will provide new insights into the molecular mechanisms that regulate mammalian sperm motility and may lead to better methods of modulating motility and thus fertility.

Acknowledgments

We thank Ping Wu for technical support.

Received November 21, 2005. Accepted July 12, 2006.

Address all correspondence and requests for reprints to: Dr. Ruey-Bing Yang, Institute of Biomedical Sciences, Academia Sinica, 128, Academia Road, Section 2, Taipei 11529, Taiwan. E-mail: rbyang@ibms.sinica.edu.tw.

This work was supported by grants from the National Science Council, Taiwan (NSC 94-2320-B-001-041 to R.B.Y. and NSC 93-2311-B-038-006 to Y.H.H.).

Disclosure of conflicts of interest: The authors have nothing to declare.

References

1. **Neill AT, Vacquier VD** 2004 Ligands and receptors mediating signal transduction in sea urchin spermatozoa. Reproduction 127:141–149
2. **Garbers DL** 1989 Molecular basis of fertilization. Annu Rev Biochem 58:719–742
3. **Cook SP, Babcock DF** 1993 Selective modulation by cGMP of the K^+ channel activated by speract. J Biol Chem 268:22402–22407
4. **Shimomura H, Dangott LJ, Garbers DL** 1986 Covalent coupling of a resact analogue to guanylate cyclase. J Biol Chem 261:15778–15782
5. **Singh S, Lowe DG, Thorpe DS, Rodriguez H, Kuang WJ, Dangott LJ, Chinkers M, Goeddel DV, Garbers DL** 1988 Membrane guanylate cyclase is a cell-surface receptor with homology to protein kinases. Nature 334:708–712
6. **Kaupp UB, Solzin J, Hildebrand E, Brown JE, Helbig A, Hagen V, Beyermann M, Pampaloni F, Weyand I** 2003 The signal flow and motor response controling chemotaxis of sea urchin sperm. Nat Cell Biol 5:109–117
7. **Matsumoto M, Solzin J, Helbig A, Hagen V, Ueno S, Kawase O, Maruyama Y, Ogiso M, Godde M, Minakata H, Kaupp UB, Hoshi M, Weyand I** 2003 A sperm-activating peptide controls a cGMP-signaling pathway in starfish sperm. Dev Biol 260:314–324
8. **Tamura N, Chrisman TD, Garbers DL** 2001 The regulation and physiological roles of the guanylyl cyclase receptors. Endocr J 48:611–634
9. **Kuhn M** 2003 Structure, regulation, and function of mammalian membrane guanylyl cyclase receptors, with a focus on guanylyl cyclase-A. Circ Res 93:700–709
10. **Schulz S, Wedel BJ, Matthews A, Garbers DL** 1998 The cloning and expression of a new guanylyl cyclase orphan receptor. J Biol Chem 273:1032–1037
11. **Kuhn M, Ng CK, Su YH, Kilic A, Mitko D, Bien-Ly N, Komuves LG, Yang RB** 2004 Identification of an orphan guanylate cyclase receptor selectively expressed in mouse testis. Biochem J 379:385–393
12. **Huang YH, Kuo SP, Lin MH, Shih CM, Chu ST, Wei CC, Wu TJ, Chen YH** 2005 Signals of seminal vesicle autoantigen suppresses bovine serum albumin-induced capacitation in mouse sperm. Biochem Biophys Res Commun 338:1564–1571
13. **Bavister BD** 1981 Substitution of a synthetic polymer for protein in a mammalian gamete culture system. J Exp Zool 217:45–51
14. **Bellve AR, Zheng W, Martinova YS** 1993 Recovery, capacitation, acrosome reaction, and fractionation of sperm. Methods Enzymol 225:113–136
15. **Wu BT, Su YH, Tsai MT, Wasserman SM, Topper JN, Yang RB** 2004 A novel secreted, cell-surface glycoprotein containing multiple epidermal growth factor-like repeats and one CUB domain is highly expressed in primary osteoblasts and bones. J Biol Chem 279:37485–37490
16. **von Wasielewski R, Werner M, Nolte M, Wilkens L, Georgii A** 1994 Effects of antigen retrieval by microwave heating in formalin-fixed tissue sections on a broad panel of antibodies. Histochemistry 102:165–172
17. **Huang YH, Chu ST, Chen YH** 1999 Seminal vesicle autoantigen, a novel phospholipid-binding protein secreted from luminal epithelium of mouse seminal vesicle, exhibits the ability to suppress mouse sperm motility. Biochem J 343(Pt 1):241–248
18. **Kitano K, Fukuda Y, Nagahira K, Nasu T, Izumi R, Kawashima K, Nakanishi T** 1995 Production and characterization of monoclonal antibodies against human natriuretic peptide receptor-A or -B. Immunol Lett 47:215–222
19. **Kitano K, Fukuda Y, Nagahira K, Nasu T, Noguchi C, Izumi R, Kawashima K, Nakanishi T** 1996 Production of polyclonal antibody specific for human natriuretic peptide receptor B. J Immunol Methods 194:147–153
20. **Chang J-C, Yang R-B, Chen Y-H, Lu K-H** 2006 A novel guanylyl cyclase receptor, BdmGC-1, is highly expressed during the development of the oriental fruit fly *Bactrocera dorsalis* (Hendel). Insect Mol Biol 15:69–77
21. **Yanagimachi R** 1994 Mammalian fertilization. In: Knobil E, Niell JD, eds. The physiology of reproduction. New York: Raven Press; 189–317
22. **Carlson AE, Westenbroek RE, Quill T, Ren D, Clapham DE, Hille B, Garbers DL, Babcock DF** 2003 CatSper1 required for evoked Ca^{2+} entry and control of flagellar function in sperm. Proc Natl Acad Sci USA 100:14864–14868
23. **Quill TA, Garbers DL** 2002 Sperm motility activation and chemoattraction. In: Hardy DM, ed. Fertilization. San Diego: Academic Press; 29–55
24. **Spehr M, Gisselmann G, Poplawski A, Riffell JA, Wetzel CH, Zimmer RK, Hatt H** 2003 Identification of a testicular odorant receptor mediating human sperm chemotaxis. Science 299:2054–2058
25. **Spehr M, Schwane K, Riffell JA, Barbour J, Zimmer RK, Neuhaus EM, Hatt H** 2004 Particulate adenylate cyclase plays a key role in human sperm olfactory receptor-mediated chemotaxis. J Biol Chem 279:40194–40203
26. **Jaiswal BS, Eisenbach M** 2002 Capacitation. In: Hardy DM, ed. Fertilization. San Diego: Academic Press; 57–117
27. **Visconti PE, Bailey JL, Moore GD, Pan D, Olds-Clarke P, Kopf GS** 1995 Capacitation of mouse spermatozoa. I. Correlation between the capacitation state and protein tyrosine phosphorylation. Development 121:1129–1137
28. **Nandi A, Mathew R, Visweswariah SS** 1996 Expression of the extracellular domain of the human heat-stable enterotoxin receptor in *Escherichia coli* and generation of neutralizing antibodies. Protein Expr Purif 8:151–159
29. **Muller D, Mukhopadhyay AK, Speth RC, Guidone G, Potthast R, Potter LR, Middendorff R** 2004 Spatiotemporal regulation of the two atrial natriuretic peptide receptors in testis. Endocrinology 145:1392–1401
30. **Quill TA, Garbers DL** 1998 Fertilization: common molecular signaling pathways across the species. In: O'Malley BW, ed. Hormones and signaling. San Diego: Academic Press; 167–207
31. **Baxendale RW, Fraser LR** 2003 Evidence for multiple distinctly localized adenylyl cyclase isoforms in mammalian spermatozoa. Mol Reprod Dev 66:181–189
32. **Blobel CP, Myles DG, Primakoff P, White JM** 1990 Proteolytic processing of a protein involved in sperm-egg fusion correlates with acquisition of fertilization competence. J Cell Biol 111:69–78
33. **Vaandrager AB, Schulz S, De Jonge HR, Garbers DL** 1993 Guanylyl cyclase C is an N-linked glycoprotein receptor that accounts for multiple heat-stable enterotoxin-binding proteins in the intestine. J Biol Chem 268:2174–2179
34. **Scheving LA, Chong KM** 1997 Differential processing of guanylyl cyclase C along villus-crypt axis of rat small intestine. Am J Physiol 272:C1995–C2004

35. **Suzuki F, Yanagimachi R** 1989 Changes in the distribution of intramembranous particles and filipin-reactive membrane sterols during in vitro capacitation of golden hamster spermatozoa. Gamete Res 23:335–347
36. **Cross NL** 1998 Role of cholesterol in sperm capacitation. Biol Reprod 59:7–11
37. **Sleight SB, Miranda PV, Plaskett NW, Maier B, Lysiak J, Scrable H, Herr JC, Visconti PE** 2005 Isolation and proteomic analysis of mouse sperm detergent-resistant membrane fractions. Evidence for dissociation of lipid rafts during capacitation. Biol Reprod 73:721–729
38. **Cross NL** 2004 Reorganization of lipid rafts during capacitation of human sperm. Biol Reprod 71:1367–1373
39. **Quill TA, Ren D, Clapham DE, Garbers DL** 2001 A voltage-gated ion channel expressed specifically in spermatozoa. Proc Natl Acad Sci USA 98:12527–12531
40. **Quill TA, Sugden SA, Rossi KL, Doolittle LK, Hammer RE, Garbers DL** 2003 Hyperactivated sperm motility driven by CatSper2 is required for fertilization. Proc Natl Acad Sci USA 100:14869–14874
41. **Ren D, Navarro B, Perez G, Jackson AC, Hsu S, Shi Q, Tilly JL, Clapham DE** 2001 A sperm ion channel required for sperm motility and male fertility. Nature 413:603–609
42. **Okunade GW, Miller ML, Pyne GJ, Sutliff RL, O'Connor KT, Neumann JC, Andringa A, Miller DA, Prasad V, Doetschman T, Paul RJ, Shull GE** 2004 Targeted ablation of plasma membrane Ca^{2+}-ATPase (PMCA) 1 and 4 indicates a major housekeeping function for PMCA1 and a critical role in hyperactivated sperm motility and male fertility for PMCA4. J Biol Chem 279:33742–33750
43. **Schuh K, Cartwright EJ, Jankevics E, Bundschu K, Liebermann J, Williams JC, Armesilla AL, Emerson M, Oceandy D, Knobeloch KP, Neyses L** 2004 Plasma membrane Ca^{2+} ATPase 4 is required for sperm motility and male fertility. J Biol Chem 279:28220–28226
44. **Shi F, Wang T** 2005 Stage- and cell-specific expression of soluble guanylyl cyclase α and β subunits, cGMP-dependent protein kinase I α and β, and cyclic nucleotide-gated channel subunit 1 in the rat testis. J Androl 26:258–263
45. **Spruill WA, Koide Y, Huang HL, Levine SN, Ong SH, Steiner AL, Beavo JA** 1981 Immunocytochemical localization of cyclic guanosine monophosphate-dependent protein kinase in endocrine tissues. Endocrinology 109:2239–2248
46. **Yuasa K, Omori K, Yanaka N** 2000 Binding and phosphorylation of a novel male germ cell-specific cGMP-dependent protein kinase-anchoring protein by cGMP-dependent protein kinase Iα. J Biol Chem 275:4897–4905
47. **Wiesner B, Weiner J, Middendorff R, Hagen V, Kaupp UB, Weyand I** 1998 Cyclic nucleotide-gated channels on the flagellum control Ca^{2+} entry into sperm. J Cell Biol 142:473–484
48. **Weyand I, Godde M, Frings S, Weiner J, Muller F, Altenhofen W, Hatt H, Kaupp UB** 1994 Cloning and functional expression of a cyclic-nucleotide-gated channel from mammalian sperm. Nature 368:859–863
49. **Foster DC, Wedel BJ, Garbers DL** 1999 Mechanisms of regulation and functions of guanylyl cyclases. Rev Physiol Biochem Pharmacol 135:1–39
50. **Pandey KN, Oliver PM, Maeda N, Smithies O** 1999 Hypertension associated with decreased testosterone levels in natriuretic peptide receptor-A gene-knockout and gene-duplicated mutant mouse models. Endocrinology 140: 5112–5119
51. **Mukhopadhyay AK, Bohnet HG, Leidenberger FA** 1986 Testosterone production by mouse Leydig cells is stimulated in vitro by atrial natriuretic factor. FEBS Lett 202:111–116

***Endocrinology* is published monthly by The Endocrine Society (http://www.endo-society.org), the foremost professional society serving the endocrine community.**